Materials at High Temperatures

ISSN: 0960-3409 (Print) 1878-6413 (Online) Journal homepage: www.tandfonline.com/journals/ymht20

Investigation on microstructure and mechanical properties of reformer furnace tube after 12 years' service

Jingfeng Guo, Tieshan Cao, Congqian Cheng & Jie Zhao

MATERIALS AT HIGH TEMPERATURES
2025, VOL. 42, NOS. 3–4, 198–207
https://doi.org/10.1080/09603409.2025.2527472

Investigation on microstructure and mechanical properties of reformer furnace tube after 12 years' service

Jingfeng Guo [a], Tieshan Cao [b], Congqian Cheng [b] and Jie Zhao [b]

[a]College of Physical Science and Technology, Yichun University, Yichun, China; [b]School of Materials Science and Engineering, Dalian University of Technology, Dalian, China

ABSTRACT

The entire reformer furnace tube is analyzed and studied through OM, SEM and mechanical property test in this work. The microstructure of centrifugal casting tube and weld joint has deteriorated, with the primary carbides coarsened and growth. The primary carbides at the dendrite boundary have grown from lamellar and skeleton shape to continuous network and chain shape, and the primary carbides M_7C_3 and Nb(Ti)C transformed into $M_{23}C_6$ and G phase. The high temperature creep strength of reformer furnace tube decreased obviously. Through the investigation of the microstructure and mechanical properties of different zones in the entire reformer furnace tube, the weakest part of the reformer furnace tube is located in the middle and lower zone, and its remnant life has been predicted. On the basis of the design temperature and pressure, the remnant life of this reformer furnace tube is 38000 hours.

ARTICLE HISTORY
Received 2 March 2025
Accepted 19 June 2025

KEYWORDS
HPNbM alloy; reformer furnace tube; remnant life; carbide; creep strength

Introduction

With the rapid development of the petrochemical industry, factors such as the reduction in raw material quality and increasing demands for product purity have driven continual improvements in production technology [1,2]. Consequently, the service environment of production equipment is evolving towards extreme working conditions, such as high temperature and high pressure [3]. In petrochemical industry, the reformer furnace tubes working at the temperature between 800 and 1000℃, and the pressure in the tube is 3-5MPa [4,5]. As catalysts deactivate, the temperature of the reformer furnace tube will exceed 1000°C during operation [6,7]. The aggressive service environment presents significant challenges to the safe operation of reformer furnace. Failure accidents occur frequently in the reformer equipment, especially the reformer furnace tubes. Therefore, the reformer furnace tube steel should show good high-temperature creep property, excellent oxidation and carburisation resistance, superior welding performance and high microstructural stability at elevated temperatures [8,9].

The materials used in reformer furnace tubes are continuously evolving. In the 1970s, the HK40 alloy for reformer furnace tubes was gradually replaced by HP40 type alloy, and now HPNbM alloy is the most widely used alloys in hydrogen reformer furnace tube [10–13]. The HPNb alloy is an HP40-type heat-resistant alloy modified by adding niobium element to form NbC carbides, which could improve the stability of the secondary phases under high-temperature service conditions. Further modified with trace amount of Ti and Zr, the HPNbM alloy exhibits a higher to creep strength and has become the new generation material for reformer and pyrolysis furnace tubes. The reformer furnace tubes made of HPNbM alloy by centrifugal casting are the core components with the highest service temperature and the most severe operating environments [14,15].

Operating long term in severe operating environments can cause significant damage or even failure in reformer furnace tubes. According to API standard 530, the high temperature reformer furnace tube is usually designed for a normal life time of 100,000 h (11.4 years) [16]. During the operation of the reformer furnace, on account of fatigue, creep, carburisation, oxidation, thermal shock, and accidental overheating premature failures of furnace tubes are frequently occurred, which pose a huge hidden danger to safety production [4,17–19]. The key damage factor of reformer furnace tube is creep damage, resulting from internal pressure and thermal stresses generated during start-up and shutdown cycles [20,21]. J. M Brear's research shows that the main load applied to the reformer furnace tube wall is the thermal stress, which caused by the periodic start-up and shutdown of the reformer furnace reduces the reformer furnace tube service life in the form of cyclic creep relaxation [22]. In addition, uneven strain caused by thermal expansion of furnace tubes can also generate thermal stress [21,23]. Moreover, the oxide layer formed on the reformer furnace tube wall during high-temperature service, which has a different thermal

CONTACT Jingfeng Guo gjf100gjf@126.com College of Physical Science and Technology, Yichun University, Yichun 336000, China; Jie zhao jiezhao@dlut.edu.cn School of Materials Science and Engineering, Dalian University of Technology, Dalian 116024, China

expansion coefficient from the reformer furnace tube material. Therefore, thermal stress is also generated during reformer furnace tube service. These thermal stresses cause further creep deformation of the furnace tubes. Overheating – occurring when the tube outer wall temperature exceeds 1000°C – is another common damage factor [24,25]. It leads to longitudinal cracking, degradation of mechanical properties, carbide aggregation, and the dissolution of fine secondary carbides in microstructure [6]. The bending of reformer furnace tube caused by overheating may also cause the phenomenon of circumferential cracking [6,26]. Therefore, the combined effect of stress gradient and thermal gradient as well as the gradient changes in microstructure of the reformer furnace wall can result in creep damage of reformer furnace tube.

The reformer furnace tube is welded from centrifugal casting heat-resistant alloy tubes. The factors that affect the service life of the reformer furnace are not only the furnace tube itself but also the weld joint [6,8]. The weld joint is generally considered to be a weak part in the reformer furnace tube [27]. Owing to uneven mechanical properties, the fusion zone of weld joint is the most prone to failure. According to reports, the cumulative creep damage at the weld joint is usually higher than other zones of the entire reformer furnace tube during normal operation. In order to improve the mechanical strength of the weld joint, the weld filler material is selected to have a chemical composition equivalent or similar to that of the base material. On another hand, the heat affected zone (HAZ) of the weld joint is other potential zone for the failure. Therefore, the microstructure evolution and the degradation of mechanical properties of weld joint are also an important factor leading to the damage of the reformer furnace tube.

Considering the importance of a long and safety operation of the reformer furnace, the microstructure characterisation and mechanical property changes of the entire reformer furnace tube (centrifugal casting tube and weld joint) need to be studied to assess the remnant service life. In this work, an entire reformer furnace tube is investigated after 12 years' service. In addition, each zone of the reformer furnace tube was studied in order to analyse the microstructure evolution and mechanical property change of centrifugal casting tube and weld joint after service.

Materials and experimental

We selected a reformer furnace tube in an ammonia plant for analysis and research, and the service time of the reformer furnace tube was 12.5 years, exceeding its design service life of 100,000 h (11.4 years). The schematic diagram of the reformer furnace tube is shown in Figure 1.

The furnace tube (centrifugal casting tubes and weld joints) in the reformer furnace are the main research objects, which is the core part of the whole reformer furnace and exposed in the highest temperature. The entire reformer furnace tube is welded from three centrifugal casting furnace tubes, divided into upper, middle, and lower sections and two weld joints. We will analyse the microstructure and properties of different positions and weld joints of the reformer furnace tube (Figure 1). The reformer furnace tube is made of HPNbM (KHR35CT) alloy produced by Kubota Corporation of Japan, with a tube specification of Φ146.6 × 9.8 mm. Table 1 is the operating condition of reformer tube.

After visual observation and dimensional inspection, samples were prepared from different zones of the entire reformer furnace tube for the microstructure and mechanical property investigations. The sampling locations for microstructure and mechanical properties are in the middle of the centrifugal casting tube. The sampling position of the upper tube section is 1.5 metres away from the upper part of weld joint 1, the sampling position of the middle tube section is in the middle of the two weld joints, and the sampling position of the lower tube section is 1.5 metres away from the lower part of weld joint 2.

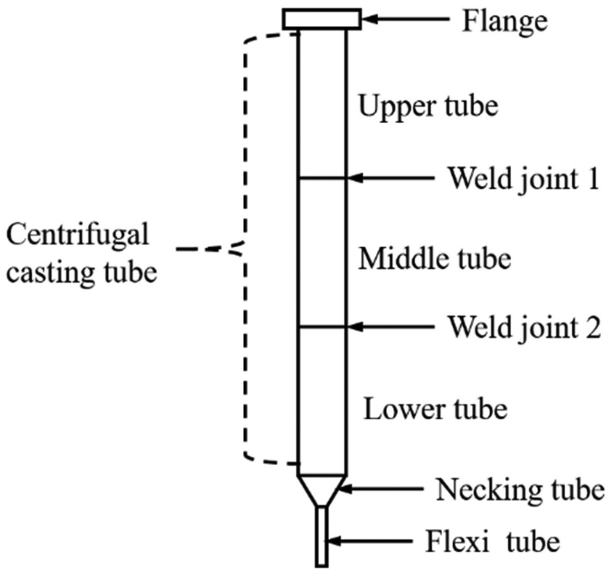

Figure 1. The schematic diagram of reformer tube.

Table 1. The operating condition of reformer furnace tube.

Item	Parameter
Feed gas flow rate	60~70t/h
Inlet temperature	603~609 °C
Outlet temperature	725~722°C
Furnace flue gas temperature	1019~1022°C
Design temperature	890°C
Outlet pressure	4.3MPa

Table 2. Chemical composition of reformer furnace tube and weld joint (wt.%).

Sample	C	Si	Mn	P	S	Cr	Ni	Mo	Nb	Ti
Kubota Standard	0.45/ 0.55	≤1.5	≤2.0	≤0.03	≤0.03	24.0/ 27.0	33.0/ 37.0	≤0.5	≤1.0	≤0.3
Upper tube	0.47	0.84	0.77	0.016	0.009	24.22	34.30	0.002	0.52	0.081
Middle tube	0.51	1.13	0.78	0.013	0.008	24.31	35.39	0.002	0.50	0.117
Lower tube	0.52	0.83	0.76	0.014	0.01	24.68	34.63	0.002	0.55	0.092
Weld joint 1	0.52	0.65	0.74	0.011	0.007	25.01	34.92	0.002	0.59	0.132
Weld joint 2	0.61	0.79	0.72	0.006	0.008	24.49	37.87	0.003	0.62	0.155

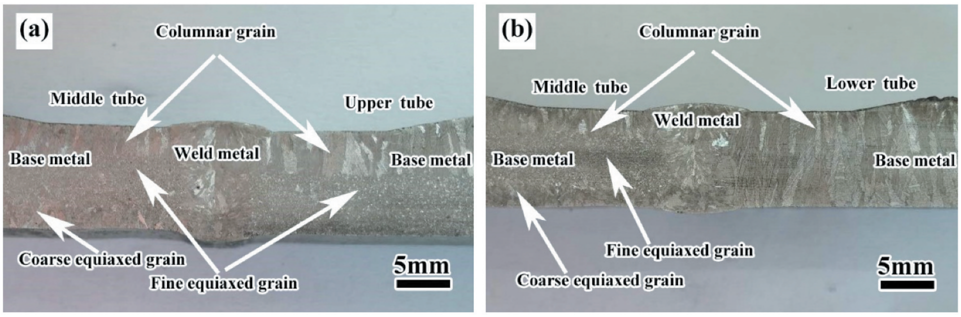

Figure 2. Macroscopic in columnar and fine equiaxed grains transverse section of the tube and weld joint: (a) weld joint 1; (b) weld joint 2.

The microstructure, room-temperature tensile properties, elevated-temperature tensile properties, and high-temperature creep properties of the reformer furnace tube were investigated by OM, SEM and tensile test. The chemical compositions of the reformer furnace tube are shown in Table 2, which are tested by Optical Emission Spectrometer (Q8 MAGELLAN). The microstructure of the sample was studied by mechanical grinding and polishing. Then, theses samples were electrolytically etched in a solution of oxalic acid (wt.10%) at 5 V, and 2A for 30 s. Microstructure characterisation was performed using SEM (Phenom Prox). The mechanical properties test specimens of centrifugal casting tube are taken in the longitudinal direction. And, the mechanical properties test specimens of weld joint are crosswelds. The room temperature tensile test of specimens with a gauge length of 35 mm is carried out a strain rate of 2.5×10^{-4}/s, which are processed according to the standard ISO 6892–1:2009 MOD. According to the standard (ISO 6892–2:2011), the elevated temperature tensile test is carried out at 1173 K with a strain rate of 0.1/min. To evaluate the creep strength at high temperature, the uniaxial creep test in tension of standard specimens (ISO 204:2009) were conducted at different temperature.

Results

Visual inspection

After visual inspection, an oxide layer was observed on the out wall of the reformer furnace tube due to servicing at high temperatures. It was determined that there were no visible cracks, holes, or other apparent damages present on the entire reformer furnace tube. No microcracks, pores, porosity, delamination and other defects were found on the surface of the reformer furnace tube after penetration testing. Measurements were taken from the three-stage reformer tube, and no significant creep expansion was detected within the furnace tube.

Macrograph

The low magnification image of the vertical section of the weld joints is shown in Figure 2. This figure illustrates the macrostructure of cross-sections from three sections of reformer tubes and two weld joints. In the upper section of the tube, the coarse columnar grains are situated on the exterior wall while fine equiaxed grains are found along its inner wall. The middle section exhibits coarse columnar grains located on its outer wall; fine equiaxed grains are positioned in between these layers within the thickness of this section's wall; and coarse equiaxed grains can be seen lining its inner wall. The macrostructure of lower tube is only coarse columnar grains. In the fusion zone, the weld metal primarily consists of columnar grains and equiaxed grains. The coarse equiaxed grains are located at the root of the weld joint. The remaining weld layers exhibit columnar grains; however, their growth direction is irregular and varies between layers. This directional inconsistency occurs because columnar grains consistently align with the direction of fastest heat dissipation during the welding process. Through the macrostructure analysis, there is no obvious defects or slag inclusions were found in the cross-sections from both weld joints and reformer furnace tubes.

Microstructure

The chemical composition of HPNbM alloy is similar to that of weld joint filler metal, which can reduce various defects during the solidification process of the weld joint (Table 2). The base metal and weld metal have a high content of C, Fe, Cr, Ni, and Nb, resulting in the formation of a large amount of carbides in base metal and weld metal. The chemical composition contains small amounts of Ti and Mo elements, which are strong carbide-forming elements. The high-temperature creep property of HPNbM alloy is improved by adding Ti element to reduce the continuity of the primary carbide at the grain boundary. The quantity and morphology of these carbides significantly influence on the mechanical properties of reformer furnace tube.

Microstructure of r as-cast reformer furnace tube and new weld joint

The microstructure of as-cast reformer furnace tube and new weld joint is shown in Figure 3. The reformer furnace tube is made by centrifugal casting, which is composed of a γ-matrix and many eutectic carbides. The primary carbide of HPNbM alloy is lamellar or skeleton shape at dendrite boundary, which is two type carbides (M_7C_3 and Nb(Ti)C) distributed on the γ matrix [28–30].

The fusion line of new weld joint in the reformer furnace tube is shown in Figure 3 (b). The fusion line is clearly defined, with numerous columnar grains growing from it into the fusion zone interior. A significant microstructural difference exists between reformer furnace tube base metal and the weld joint fusion zone, the fusion zone exhibits a notably higher carbide content and smaller carbide size.

The microstructure of the weld metal in new weld joint is a typical cast dendritic structure composed of cellular and columnar grains, with columnar grains growing along the direction of fastest heat dissipation (Figure 3 (c)). In Figure 3, it can be seen that the primary carbides in the weld metal of the weld joint are very fine, and the primary carbides are distributed in a skeleton shape along the grain boundaries.

Microstructure of reformer furnace tube after 12 years' service

The microstructure of reformer furnace tube after 12 years' service is shown in Figure 4. The working temperature of reformer furnace tubes varies from 800

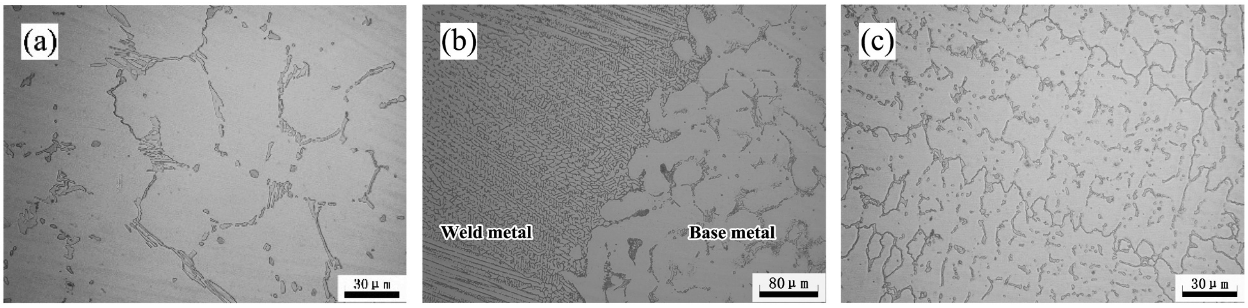

Figure 3. Microstructure of cast tube and new weld joint: (a) reformer furnace tube (base metal), (b) fusion line, (c) weld metal.

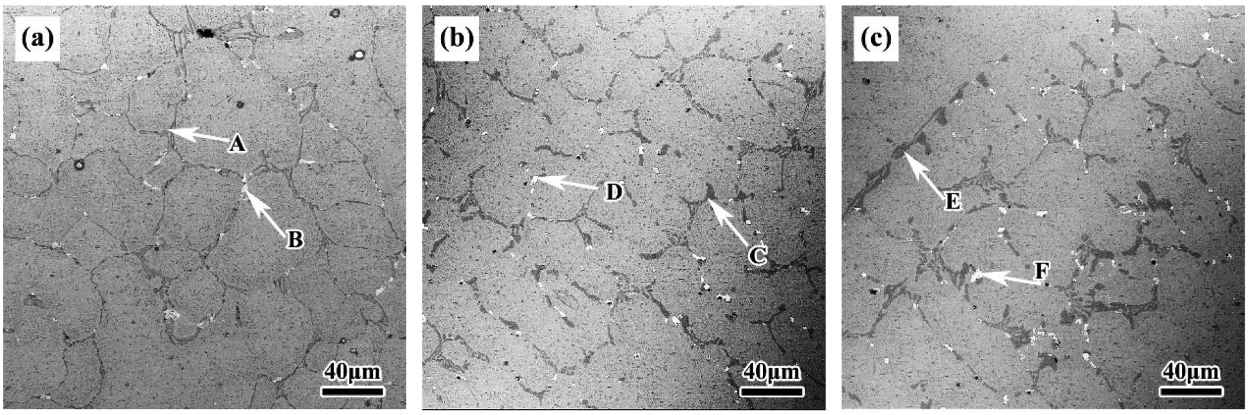

Figure 4. Microstructure of the reformer furnace tube: (a) upper tube, (b) middle tube, (c) lower tube.

to1000℃. After 12 years' service, there are a large number of fine secondary carbides precipitated in dendrite interior. The primary carbides coarsened and formed a continuous network in the reformer furnace tube. Moreover, the crystal structure of carbides also undergoes transformation at high temperatures. The primary M_7C_3 type carbides changed into $M_{23}C_6$ type carbides [28,31,32]. The Nb(Ti)C is unstable above 900°C and tends to transform into G-phase (nickel-niobium silicide) [7,33–35]. Si element has a major part to play in G phase transformation, promoting the transformation of Nb carbides into brittle G phases. However, Ti is able to inhibit the transformation of Nb carbides into G-phase and hold the alloy high-metallurgical stability.

The chemical composition of carbide of the serviced reformer furnace tube was investigated by EDS in Figure 4. The chemical composition of carbides in Figure 4 is shown in Table 2. There are two types of carbides in the reformer furnace tube: Cr-rich carbides $M_{23}C_6$ and Nb-rich carbides G phase with some Ni and Si. The grey carbide is $M_{23}C_6$ type carbide and the bright carbides is G phase (Figure 4). The primary chromium carbide of M_7C_3 with HCP crystalline structure (Pnma) transformed to $M_{23}C_6$ with FCC structure(Fm-3 m) after service (Figure 4). The primary niobium carbide of Nb(Ti)C with BCC structure(Fm-3 m) changed into G phases with FCC structure(Fd-3 m) in HPNbM alloy after 12 years' service.

Microstructure of weld joint after 12 years' service

Figure 5 shows the microstructure at the fusion line of weld joint. The fusion line remains clearly defined, but there are a large of fine carbides precipitated in grain interior of base metal and weld metal. Previous research has demonstrated that these precipitated carbides are $M_{23}C_6$ type carbides [15,36,37]. The precipitation and growth of secondary carbides in grain interior reduced the microstructural differences between weld metal and base metal, thereby decreasing the differences in mechanical properties of these two zones. Figure 6 presents the microstructure of the weld joint fusion zone in reformer furnace tube. Similar to the reformer furnace tube itself, many fine secondary carbides are precipitated at the dendrites of weld metal. The primary carbides in weld metal also underwent coarsen and a crystal structure transformation as in reformer furnace tube, which will not be further described here. In the process of high-temperature service, the primary carbide of base metal and weld metal was transformed and coarsened, and a large amount of fine secondary carbides were precipitated

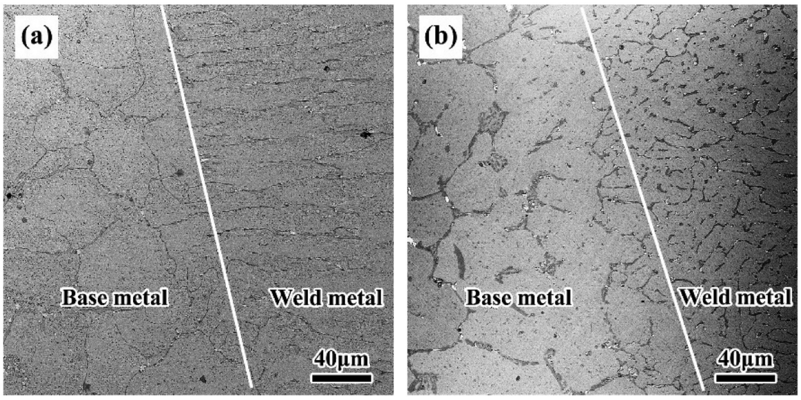

Figure 5. Microstructure of weld joint fusion line: (a) weld joint 1(upper), (b) weld joint 2(lower).

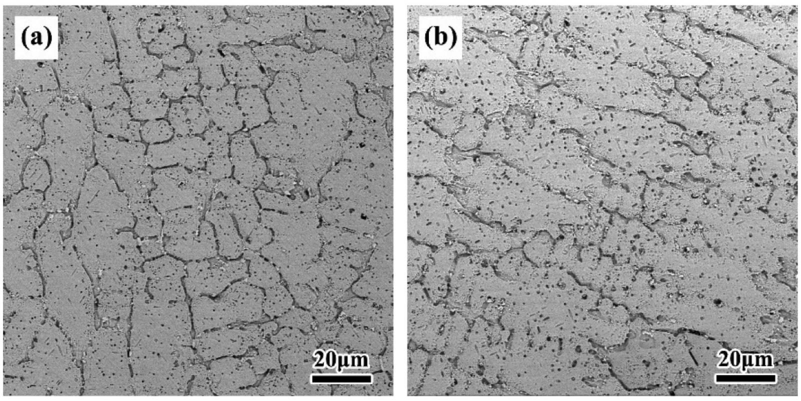

Figure 6. Microstructure of weld joint fusion zone: (a) weld joint 1(upper), (b) weld joint 2(lower).

in the dendrites, which causes the deterioration of the microstructure of reformer furnace tube and weld joint.

Mechanical properties

Reformer furnace tubes are serviced in severe environments with high temperature and high carbon. Therefore, the high temperature mechanical properties are very important for the application of reformer furnace tube, especially the creep property at elevated temperature play a key role in service life. The mechanical properties of the reformer furnace tube and weld joint at room temperature and high temperature were studied in this work.

Tensile test at room temperature

Table 3 shows the tensile properties of reformer furnace tube and weld joint at room temperature. The tensile strength of the serviced reformer furnace tube and weld joint is more than 500 MPa, the yield strength is about 300MPa, and the elongation is only 4.0%. The serviced tubes and weld joints exhibited a higher tensile strength and yield strength than cast tube as a result of many fine secondary carbides in the dendrite interior. At the same time, due to a continuous network of the primary carbides is at grain boundary, the ductility is lower than cast tube after service. The fracture positions of both the new weld joint and the serviced weld joint are located in weld metal, indicating that the weld fusion zone is still the weak part of the weld joint even after service.

Tensile test at high temperature

Table 4 shows the tensile strength of reformer furnace tube and weld joint at 900°C. The tensile strength of the serviced reformer furnace tube and weld joint is higher than cast tube, the yield strength is lower than cast tube, and the elongation is similar for each other. The high temperature tensile strength of the middle tube and weld joint 2 are similar, significantly lower than the other three zones. They are all in the lower central zone of the entire reformer furnace tube (Table 5). The continuous carbide at grain boundary could decrease the strength of reformer furnace tube at high temperature. The failure location of both the new weld joint and the serviced weld joint are still situated in weld metal even at elevated temperature tensile test.

Accelerated creep test at high temperature

The creep strength of the reformer furnace tube and weld joint at high temperature is shown in Table 6. The corresponding creep data points for both the furnace tube and weld joint were plotted on the Larson-Miller (L-M) curve (Figure 7). All the plotted points situate below the minimum creep strength curve for the HPNbM alloy, which indicates that their creep strength is lower than the minimum creep strength. The coarsening and growth of primary carbides in reformer furnace tube result in the disappearance of lamellar or skeleton shape of carbides at grain boundaries, which are replaced by chain or network shape. The lamellar or skeleton shape of carbide at grain boundary increases the tortuosity of grain boundaries, lead to dislocations move difficult during creep and improved the creep strength of the alloy. However, the chain and network morphology of grain boundary carbides reduces the tortuosity of grain boundaries, making it easier for dislocations to move during creep, resulting in a decrease in the creep property of serviced reformer furnace tube. The creep rupture time of the middle tube zone at different temperature is the shortest in the entire reformer furnace tube (Table 6). Therefore, the middle tube is the weakest zone of the entire reformer furnace tube. The failure location of the specimens in the high-temperature creep test of weld joint are in weld metal and the fusion line, indicating that

Table 3. Chemical composition of second phase (wt.%).

Sample	C	Fe	Cr	Ni	Si	Nb	Ti
A	8.38	36.78	18.60	35.39	0.85		
B	11.02	15.99	8.56	39.83	6.33	18.27	
C	11.76	6.55	73.17	6.18	1.67	0.99	
D	12.11	7.07	72.14	6.21	0.71	1.76	
E	13.47	26.88	29.47	29.56	0.61		
F	16.21			45.59	7.90	27.77	2.54

Table 4. The tensile strength of reformer furnace tube and weld joint at room temperature.

Sample	Rm (MPa)	$Rp_{0.2}$ (MPa)	A (%)	Failure location
Cast tube	550±5	282±2	15.5±3	
Upper tube	537±4	313.1±3.2	4.2±0.6	
Middle tube	561.4±12.5	300.4±2.3	4.6±0.1	
Lower tube	541.9±0.4	302.3±2.7	4.4±0.3	
New weld joint	585±20	322±12	8±2	weld metal
Weld joint 1	562.1±3.6	322.5±2	4.0±0.	weld metal
Weld joint 2	531.9±11.2	298.1±7.9	4.7±0.1	weld metal

Table 5. The mechanical properties of reformer tubes and weld joints at high temperature.

Sample	Temperature(°C)	Rm (MPa)	$Rp_{0.2}$ (MPa)	A (%)	Failure location
Cast tube	900	165±5	137±6	36±5	
Upper tube	900	181±2	92±1.5	32.3±5.3	
Middle tube	900	167±1	84.8±0.7	37.8±1.3	
Lower tube	900	176±0	87.8±0.8	46.3±2.3	
New weld joint	900	200±6	105±7	27±3	weld metal
Weld joint 1	900	182±3	90.3±2.3	28.3±2.3	weld metal
Weld joint 2	900	167.5±1.5	84.8±0.8	43±0.5	weld metal

Table 6. The accelerated creep test of reformer furnace tube and weld joint at high temperature.

Sample	Temperature(°C)	Stress (MPa)	Rupture time (h)	Failure location
Upper tube	900	60	244.2	
	1000	45	27.19	
Middle tube	900	60	86.6	
	1000	45	4.88	
Lower tube	900	60	116	
	1000	45	9.54	
Weld joint 1	900	60	122.9	weld metal
	1000	45	16.31	weld metal
Weld joint 2	900	60	100.28	weld metal
	1000	45	10.69	Fusion line

the weld fusion zone remains a relatively weak part in the weld joint during service.

Discussion

As revealed by the microstructural and mechanical properties analysis, the degree of microstructural degradation across three zones of the reformer furnace tube is similar, with no significant differences observed. The microstructure of the weld joints at both positions is also similar. However, the high-temperature mechanical properties vary significantly in different zones, especially in the middle and lower region of the entire reformer furnace tube. The creep strength is the lowest, which is the key position for the evaluation of the remnant life of the reformer tube. Similar to the 'barrel theory' (where the shortest stave determines capacity), the service life of the entire reformer furnace tube is determined by the weakest area. Therefore, this work focuses on conducting creep rupture tests on the weak zone of the reformer furnace tube in order to predict its remnant life. The service life of reformer furnace tube mainly depends on its creep strength. As the weakest zone, a series of high-temperature creep rupture test were conducted on the middle tube in this work. In order to accelerate the creep experiment, we choose creep test stress and temperature higher than the reformer furnace tube working stress and temperature. These creep tests were conducted within the temperature range of 900–1020°C and the stress range of 27–60 MPa (Table 7). According to the fitted curve of this data band, the remnant life of the reformer furnace tube was calculated and predicted (Figure 7). For this HPNbM alloy in this work, Larson-Miller Parameter (LMP): $p = T\times(23+\log t_r)\ \times 10^{-3}$. Where T is the absolute temperature in K and t_r is the rupture time in hours.

Stress and design life analysis of reformer tube

According to the data provided by the chemical plant, the design operating temperature of the reformer furnace tube is 890℃, the working pressure is 4.3 MPa, the outer diameter of the tube is 146.6 mm (OD), and the wall thickness of dense layer is 9.8 mm. The following formula is the hoop stress σ_h acting on reformer furnace tube, which is calculated to predict the remnant life:

$$\sigma_h = P_o \times (OD - \delta)/(2 \times \delta) \qquad (1)$$

Where P_o is the operating pressure in MPa, OD is the mean outer diameter in mm and δ is the thickness of the tube in mm. And,

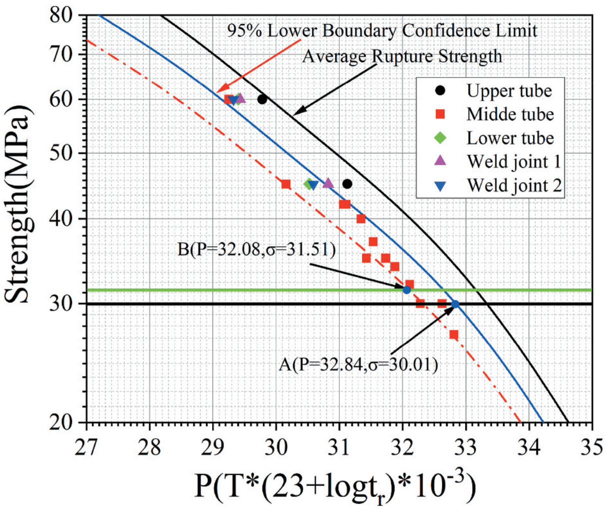

Figure 7. The stress versus LMP of HPNbM alloy (P=T×(23+logtr)×10^{-3}) [38].

Table 7. The accelerated creep test of reformer furnace tube at high temperature (middle tube).

Sample	Temperature(°C)	Stress (MPa)	Rupture time (h)	P value
1	900	60	86.6	29.25
2	1000	45	4.88	30.16
3	930	37	1636	31.54
4	930	42	714.7	31.10
5	955	35	690	31.73
6	955	40	333.5	31.34
7	955	42	197.3	31.06
8	970	35	191.5	31.43
9	970	34	440.2	31.88
10	1000	30	227	32.28
11	1000	32	167.6	32.118
12	1020	27	237.7	32.818
13	1020	30	169.6	32.628

$$\sigma_h = P_o \times (OD - \delta)/2 \times \delta = 4.3 \times (146.6 - 9.8)/2 \times 9.8 = 588.24/19.6 = 30.01\text{MPa} \quad (2)$$

The horizontal line of 30.01 MPa intersects with the lower line of the L-M curve of HPNbM alloy at point A, corresponding to a p value of 32.84 (Figure 7). Based on the reverse calculation of the design operating temperature of 890 ℃, the design life at this temperature is calculated to be 172,307 h, which means the service life of the designed reformer furnace tube is approximately over 170,000 h.

Remnant life analysis of reformer furnace tube after service

During service, the effective wall thickness of the reformer furnace tube is bound to decrease due to the damage mechanisms such as oxidation and decarburisation. The designed wall thickness of the dense layer for the furnace tube is 9.8 mm. Given that both the oxidation corrosion and decarburisation layers on the inner and outer walls are minimal, and considering the limitations associated with actual measurements, a safety margin has been applied: 0.2 mm will be deducted from the inner layer and 0.3 mm from the outer layer, resulting in a total deduction of 0.5 mm for the corrosion-affected layer.

When calculating the minimum effective wall thickness, effective diameter and hoop stress is:

$$\delta = 9.8 - 0.5 = 9.3\text{mm} \quad (3)$$

$$\text{OD} = 146.6 \times (2 \times 0.5) = 145.6\text{mm} \quad (4)$$

$$\sigma_h = Po \times (OD - \delta)/(2 \times \delta) = 4.3 \times (145.69.3)/(2 \times 9.3) = 31.51\text{MPa} \quad (5)$$

It intersects the bottom line of the fitted curve at point B, and the p value is 32.08. If the design temperature is 890℃, the t_r is about 38,356 h according to the formula $P=T\times(23+\log t_r)\times10^{-3}$. Therefore, the remnant life of this reformer furnace tube is more than 38,000 h. The reformer furnace tube can still run for another working cycle.

Conclusion

Through visual observation and macroscopic inspection, there is no obvious damages on outer wall of the entire reformer tube. And, the microstructure and mechanical property of HPNbM alloy reformer furnace tube are analysed in present work. The following conclusions are follows:

(1) The microstructure of the reformer furnace tube has deteriorated, with the primary carbide coarsened and aggregation growth. The primary carbides at the grain boundary have grown from lamellar and skeletal shape to continious network or chain shape, and the crystal structure has also undergone a transformation. At the same time, a large amount of fine secondary carbides precipitate in dendrite interior.

(2) After a long time service, the ductility of reformer furnace tubedecreases and the brittleness increases. In particular, the mechanical properties of high temperature decrease greatly. The high-temperature creep strength of furnace tube decreased obviously.

(3) By studying the microstructure and mechanical properties of different zones of the entire reformer tube, the weakest part of the reformer furnace tubeis located in the middle tube, and its remnant life has been predicted. According to the design temperature and pressure of the reformer, there are still 38,000 h of remnant life for this reformer furnace tube.

Disclosure statement

No potential conflict of interest was reported by the author(s).

Funding

This research was supported by Jiangxi Provincial Natural Science Foundation of China [Grant No. 20232BAB204005].

ORCID

Jingfeng Guo http://orcid.org/0000-0001-9338-424X

References

[1] Xuqian C, Yun L, Yunkai C, et al. Failure analysis of overheated coil leakage in ethylene cracking furnace. Eng Fail Anal. 2023;152:107465. doi: 10.1016/j.engfailanal.2023.107465
[2] Shifeng X, Jielu W, Chaopeng H, et al. Failure analysis of convection section tube in an ethylene cracking furnace due to metal dusting. Eng Fail Anal. 2023;154:107642. doi: 10.1016/j.engfailanal.2023.107642
[3] Gudenko AS, Skorobogatykh VN, Korneev AA, et al. Effect of the operating temperature of a steam methane reforming furnace on structural changes and crack susceptibility in welding 800ht nickel alloy. Metallurgist. 2023;67(1–2):17–24. doi: 10.1007/s11015-023-01485-5
[4] Rampat K, Maharaj C. Creep embrittlement in aged Hp-Mod alloy reformer tubes. Eng Fail Anal. 2019;100:147–165. doi: 10.1016/j.engfailanal.2019.02.022
[5] Buchanan KG, Kral MV. Crystallography and morphology of niobium carbide in as-cast HP-Niobium reformer tubes. Metall Mater Trans A. 2012;43A(6):1760–1769. doi: 10.1007/s11661-011-1025-0
[6] Attarian M, Taheri AK, Jalilvand S, et al. Microstructural and failure analysis of welded primary reformer furnace tube. Made of Hp-Nb micro alloyed heat resistant steel. Eng Fail Anal. 2016;68:32–51. doi: 10.1016/j.engfailanal.2016.05.023
[7] Mostafaei M, Shamanian M, Purmohamad H, et al. Microstructural degradation of two cast heat resistant reformer tubes after long term service exposure. Eng Fail Anal. 2011;18(1):164–171. doi: 10.1016/j.engfailanal.2010.08.017
[8] Gang L, Qun C, Xiaofeng L, et al. Failure analysis of cracking in the welded joints of hydrogen reformer outlet pigtail tubes. Eng Fail Anal. 2022;137:106257. doi: 10.1016/j.engfailanal.2022.106257
[9] Mostafaei M, Shamanian M, Purmohamad H, et al. Increasing weldability of service-aged reformer tubes by partial solution annealing. J Materi Eng Perform. 2016;25(4):1291–1303. doi: 10.1007/s11665-016-1973-z
[10] Wu XQ, Jing HM, Zheng YG, et al. The eutectic carbides and creep rupture strength of 25cr20ni heat-resistant steel tubes centrifugally cast with different solidification conditions. Mater Sci Eng a-Struct Mater Prop Microstructure Process. 2000;293(1–2):252–260. doi: 10.1016/S0921-5093(00)00984-9
[11] de Almeida LH, Ribeiro AF, Le May I. Microstructural characterization of modified 25cr-35ni centrifugally cast steel furnace tubes. Mater Charact. 2002;49(3):219–229. doi: 10.1016/S1044-5803(03)00013-5
[12] Andrade AR, Bolfarini C, Ferreira LAM, et al. Influence of niobium addition on the high temperature mechanical properties of a centrifugally cast HP alloy. Mater Sci Eng a-Struct Mater Prop Microstructure Process. 2015;628:176–180. doi: 10.1016/j.msea.2015.01.049
[13] Andrade AR, Bolfarini C, Ferreira LAM, et al. Titanium micro addition in a centrifugally cast hpnb alloy: high temperature mechanical properties. Mater Sci Eng a-Struct Mater Prop Microstructure Process. 2015;636:48–52. doi: 10.1016/j.msea.2015.03.085
[14] Bonaccorsi L, Guglielmino E, Pino R, et al. Damage analysis in Fe-Cr-Ni centrifugally cast alloy tubes for reforming furnaces. Eng Fail Anal. 2014;36:65–74. doi: 10.1016/j.engfailanal.2013.09.020
[15] Alvino A, Lega D, Giacobbe F, et al. Damage characterization in two reformer heater tubes after nearly 10 years of service at different operative and maintenance conditions. Eng Fail Anal. 2010;17(7–8):1526–1541. doi: 10.1016/j.engfailanal.2010.06.003
[16] Gong JM, Tu ST, Yoon KB. Damage assessment and maintenance strategy of hydrogen reformer furnace tubes. Eng Fail Anal. 1999;6(3):143–153. doi: 10.1016/S1350-6307(98)00042-9
[17] Swanepoel DB, Eschbach K. Embrittlement of Hp40nb heat-resistant alloy at intermediate operating temperatures. J Fail Anal Preven. 2021;21(4):1133–1142. doi: 10.1007/s11668-021-01168-w
[18] Han Z, Xie G, Cao L, et al. Material degradation and embrittlement evaluation of ethylene cracking furnace tubes after long term service. Eng Fail Anal. 2019;97:568–578. doi: 10.1016/j.engfailanal.2019.01.041
[19] Ilman MNK. Analysis of material degradation and life assessment of 25Cr–38Ni–mo–Ti wrought alloy steel (Hpm) for cracking tubes in an ethylene plant. Eng Fail Anal. 2014;42:100–108. doi: 10.1016/j.engfailanal.2014.03.020
[20] El-Batahgy A, Zaghloul B. Creep failure of cracking heater at a petrochemical plant. Mater Charact. 2005;54(3):239–245. doi: 10.1016/j.matchar.2004.12.014
[21] Hoerner M, Sheth P, Corleto C. Failure analysis of a furnace shell in a petrochemical plant. J Fail Anal Preven. 2023;23(6):2315–2321. doi: 10.1007/s11668-023-01791-9
[22] Brear JM, Church JM, Humphrey DR, et al. Life assessment of steam reformer radiant catalyst tubes — the use of damage front propagation methods. Int J Press Vessels Pip. 2001;78(11–12):985–994. doi: 10.1016/S0308-0161(01)00113-2
[23] Young DJ, Zhang J. Carbon corrosion of alloys at high temperature. J South Afr Inst Min Metall. 2013;113(2):153–158.
[24] Swaminathan J, Prasad P, Gunian MK, et al. mechanical strength and microstructural observations for remaining life assessment of service exposed 24Ni-24Cr-1.5Nb cast austenitic steel reformer tubes. Eng Fail Anal. 2008;15(6):723–735. doi: 10.1016/j.engfailanal.2007.06.009
[25] Ray AK, Sinha SK, Tiwari YN, et al. Analysis of failed reformer tubes. Eng Fail Anal. 2003;10(3):351–362. doi: 10.1016/S1350-6307(02)00029-8
[26] Guglielmino E, Pino R, Servetto C, et al. Damage investigation on welded tubes of a reforming furnace. Metallurgia Ital. 2015;1:53–58.

[27] Guo JF, Cao TS, Cheng CQ, et al. Evaluation of creep rupture behaviour for weld joint and base metal of the Cr35ni45nb alloy. Sci Technol Weld Joining. 2018;23 (6):449–453. doi: 10.1080/13621718.2018.1432107

[28] Kondrat'ev SY, Kraposhin VS, Anastasiadi GP, et al. Experimental observation and crystallographic description of M7C3 carbide transformation in Fe–Cr–Ni–C HP type alloy. Acta Materialia. 2015;100:275–281. doi: 10.1016/j.actamat.2015.08.056

[29] Kenik EA. Structure and phase stability in a cast modified-hp austenite after long-term ageing. Scr Materialia. 2003;49(2):117–122. doi: 10.1016/S1359-6462(03)00238-0

[30] Nunes FC, Dille J, Delplancke JL, et al. Yttrium addition to heat-resistant cast stainless steel. Scr Materialia. 2006;54(9):1553–1556. doi: 10.1016/j.scriptamat.2006.01.024

[31] Kraposhin VS, Kondrat'ev SY, Talis AL, et al. Experimental investigation of in-situ transformations of the M 7C3 carbide in the cast Fe–Cr–Ni alloy. Phys Met Metallogr 2017;118(3):227–232. doi: 10.1134/S0031918X17030085

[32] Liu C, Chen X, Chen T, et al. Carbide transformation in carburised zone of 25Cr35NiNb+Ma alloy after high-temperature service. Mater High Temperatures. 2016;33(1):98–104. doi: 10.1080/09603409.2015.1130330

[33] Sosa Lissarrague MHL, Armando C. Nbc transformation during aging in Hp40-Nb heat resistant alloy. Acta Metall Slovaca. 2022;28(3):147–150. doi: 10.36547/ams.28.3.1562

[34] Kondrat'ev SY, Sviatysheva EV, Anastasiadi GP, et al. Fragmented structure of niobium carbide particles in as-cast modified Hp alloys. Acta Materialia. 2017;127:267–276. doi: 10.1016/j.actamat.2017.01.043

[35] Zhang YH, Li M, Godlewski LA, et al. Creep behavior at 1273 K (1000 °C) in Nb-bearing austenitic heat-resistant cast steels developed for exhaust component applications. Metall Mater Trans A. 2016;47A (7):3289–3294. doi: 10.1007/s11661-016-3544-1

[36] Guo J, Cao T, Cheng C, et al. Microstructure evolution and mechanical properties degradation of HPNb alloy after a five-year service. Mater Res Express. 2018;5(4):046509. doi: 10.1088/2053-1591/aab8e9

[37] Swaminathan J, Guguloth K, Gunjan M, et al. Failure analysis and remaining life assessment of service exposed primary reformer heater tubes. Eng Fail Anal. 2008;15(4):311–331. doi: 10.1016/j.engfailanal.2007.02.004

[38] NRIM creep data sheet No. 38A, Data sheets on the elevated temperature properties of centrifugally cast tubes and cast block of 25Cr·35Ni·0.4C steel for reformer furnaces (SCH 24).